# Characteristics of sealed plasma electrolytic oxidation coatings with electrochemical impedance spectroscopy*

Lü Guo-Hua(吕国华)[a)†], Chen Huan(陈 晥)[a)], Wang Xing-Quan(王兴权)[b)], Pang Hua(庞 华)[a)], Zhang Gu-Ling(张谷令)[b)], Zou Bin(邹 斌)[b)], Lee Heon-Ju[c)], and Yang Si-Ze(杨思泽)[a)]

[a)] *Beijing National Laboratory for Condensed Matter Physics, Institute of Physics, Chinese Academy of Sciences, Beijing* 100190, *China*
[b)] *College of Science, Minzu University of China, Beijing* 100081, *China*
[c)] *Faculty of Mechanical & Energy System Engineering, Cheju National University, Cheju* 690756, *Korea*

(Received 20 January 2010; revised manuscript received 19 February 2010)

Plasma electrolytic oxidation (PEO) coatings are prepared on aluminium with graphite powders added into the electrolyte. The scanning electron microscopy (SEM) coupled with an energy dispersive x-ray analysis system (EDX) is used to characterize the surface and the cross-section morphologies of the coatings. The electrochemical impedance spectroscopy (EIS) is used not only to evaluate the corrosion resistance but also to analyse the structure of the coating. Results show that graphite powders are embedded in the PEO coating. The corrosion resistances of both the inner barrier and the outer porous layer are greatly improved, and the EIS could give some valuable detailed information about the coating structure.

**Keywords:** plasma electrolytic oxidation, electrochemical impedance spectroscopy, coating, additives

**PACC:** 5280W, 8245, 8160

## 1. Introduction

Plasma electrolytic oxidation (PEO) technique is increasingly gaining attention as a novel technique for surface modification of valve metals such as Al, Mg, Ti and their alloys.[1−3] It is a complex process combining electrochemical oxidation with gas evolution, dielectric breakdown, oxide film formation and dissolution.[1,4] During the PEO process, sparking discharge is one of the key features when the voltage exceeds a critical breakdown value.[5] This results in high temperature and pressure in the discharge channels, which can reach 6800–9500 K and $10^2$–$10^3$ MPa, respectively.[1] Simultaneously, a series of complicated and violent physical–chemical reactions take place in the channels where coatings with high mechanical properties and high growth rate are produced.[6,7] However, sparking discharge and short annealing effect result in micro-pores and micro-cracks in the coatings. The porous structure may extend the usage of the coating to serving as decorative material after being coloured, but this can reduce the corrosion resistance of PEO coatings under wicked conditions such as in sea water.[8]

Therefore, one of the main challenges to the PEO technique is to seal the porous layer of the coatings. Hydrothermal sealing (HTS) is well developed for sealing traditional anodic coatings,[9,10] but few reports to deal with the PEO coatings can be found. In recent years, some multi-immersion techniques are applied to the enhancement of the PEO coatings.[11] However, they are somewhat inconvenient in use, for their process is complicated. Since PEO process is accompanied with diffusion and electrophoresis of the electrolyte elements, it is thought that additives in the electrolyte may participate in the reactive process and turned into a part of the coating.[12,13] Tong *et al.*[14] and Jin *et al.*[15] added nano-powders such as $SiO_2$ and Fe into the electrolyte and found that the nanograins could be embedded in the ceramic coatings and the corresponding coatings were less porous. Nie *et al.*[16] added graphite into the electrolyte and the wear resistance of the PEO coatings was improved. Our previous paper[17] reported that adding graphite powders with an appropriate size into the electrolyte could improve the corrosion resistance of PEO coatings.

Obviously, adding powders with an appropriate size into the electrolyte is a convenient and effective

*Project supported by the Funds for International Cooperation and Exchange of the National Natural Science Foundation of China (Grant No. 10811140326) and the State Key Program of the National Natural Science Foundation of China (Grant No. 10735090).
†Corresponding author. E-mail: lvguohua@aphy.iphy.ac.cn
© 2010 Chinese Physical Society and IOP Publishing Ltd

way to seal the porous layer of PEO coatings. However, the above reports only mentioned the additive effect but did not give any detailed analysis of the reactive process. Electrochemical impedance spectroscopy (EIS) can give not only electrochemical properties but also some structure information about the coatings. It has been used as a powerful tool for obtaining detailed information about the auto sealing and the ageing process of anodized aluminum.[9,10]

In the present work, the EIS is used to study the characteristics of the graphite sealed PEO coatings: the EIS is used for both the sealed and unsealed PEO coatings. The experimental EIS result is modeled by the equivalent electrical circuit with the corresponding electrical parameters given. The detailed information about the growth process for the sealed PEO coatings is also explained.

## 2. Experiment

Rectangular samples of pure Al (0.005 wt% Cu, 0.003 wt% Fe, and 0.0025 wt% Si, Al-balance) with a dimension of 20 mm × 20 mm × 0.3 mm were used as the working electrode and a stainless steel bar as the counter one in the experiment. Prior to the PEO treatment, the samples were ground down to 800# SiC paper, then they were degreased in acetone and distilled water sequentially. The PEO processes were carried out with a conventional plasma electrolytic oxidation unit composed of a pulsed DC source with 100-Hz modulation, a stirring system and a cooling system. An aqueous solution was prepared with the mixed composition of 0.03 M $Na_2SiO_3$+0.05 M NaOH. Graphite powders with an average diameter of 10 $\mu$m as shown in Fig. 2(a), were added into the electrolyte at a density of 5 g/l. On account of the hydrophobic nature, the graphite powders were degreased in trichloroethylene and cleaned with dilute nitric acid, then added into the electrolyte and stirred uniformly. The current density in the oxidation process was maintained constantly at approximately 5 A/dm$^2$, and the temperature of the electrolyte was kept below 35 °C. The treatment time was 30 min. In addition, samples produced in the electrolyte without graphite were used for comparison.

The voltage–time responses were recorded by the Tektronix TDS 2012 digital storage oscillograph in the PEO process. The surface and the cross-section morphologies and the element distribution of the coatings were examined by scanning electron microscopy (SEM, HITACH S-4200) coupled with an energy dispersive x-ray analysis system (EDX). The surfaces of all the samples used for the SEM study were coated with a thin gold layer in order to prevent the surface charging effect.

The electrochemical measurements were carried out in a 3.5-wt% NaCl solution. A three-electrode system was employed with the sample serving as a working electrode, saturated calomel electrode (SCE) as a reference electrode and platinum as the counter electrode. Samples used in the electrochemical test were embedded within epoxy resin, with an exposed area of 1 cm$^2$ retained. Before the electrochemical test, all the samples were immersed in the 3.5-wt% NaCl solution for 10 min. The EIS spectrum was collected by using EG&Par frequency response detector (Model 1025) with M398 software. The signal amplitude of EIS was 5 mV and the frequency ranged between $10^{-2}$ and $10^5$ Hz.

## 3. Results and discussion

### 3.1. Voltage–time responses

Voltage–time responses of the PEO processes with and without graphite additives are shown in Fig. 1.

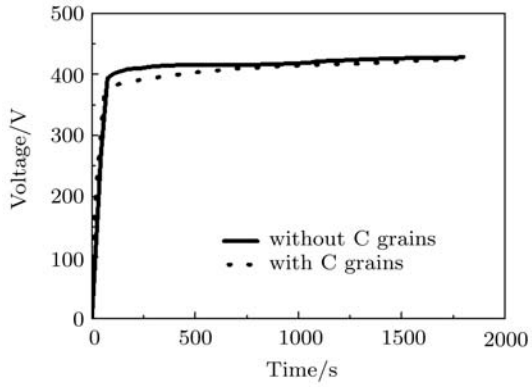



**Fig. 1.** Voltage–time response for the coatings with and without graphite additives.

Both the processes have two voltage stages. In the first stage the voltages both increase very quickly to more than 300 V, while in the second stage they increase slowly and become almost constant in the end. At the turning point of the two stages, the voltage with graphite additives in the electrolyte was lower than that without graphite additives. As is well known, the first stage is the traditional anodic oxidation stage and the second is the sparking stage. The voltage at the

turning point is called the breakdown voltage. Therefore, figure 1 indicates that the breakdown voltage of the PEO process becomes lower with graphite powder additives in the electrolyte. This is attributed to the higher electric conductivity of the electrolyte which is induced by the conductivity of the graphite powders.

## 3.2. Morphologies of the PEO coatings

Figures 2(b) and 2(c) show the surface micrographs of the PEO coatings without and with graphite additives in the electrolyte, respectively. Typical coating morphologies such as micro-pores and pan-like structures are observed. Coatings with graphite additives in the electrolyte seem more uniform and much denser than those without additives. This is attributed to the embedment of the graphite in the pores of the coatings as we have reported in Ref. [17].

Figure 3 shows the cross-section morphology and the element distribution across the coating produced in the electrolyte with graphite powder additives. The cross section of the coating seems compact, and no two-layer structure is found clearly. The element distribution images indicate that graphite powders in the electrolyte participate in the oxidation process and are distributed all over the coating cross section. In addition, the powders prefer to be distributed in the surface of the coating. As we have discussed in Ref. [17], the distribution of the graphite powders was greatly influenced by the pore size and most of them were distributed around the pore area. With the oxidation going on, the pores size became larger. This made it easier for the powders to be imbedded inside, therefore more carbon elements could be found in the surface of the coating.

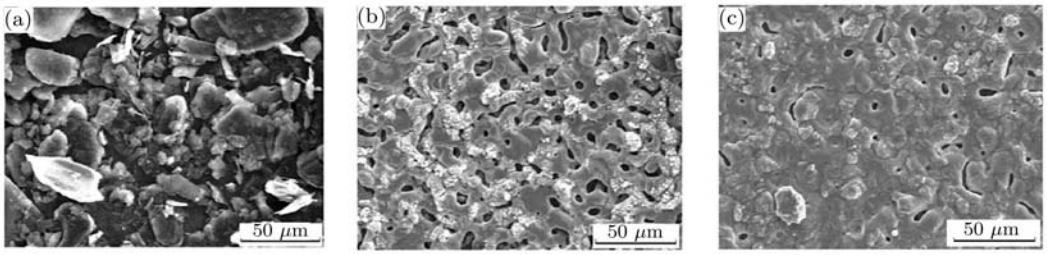
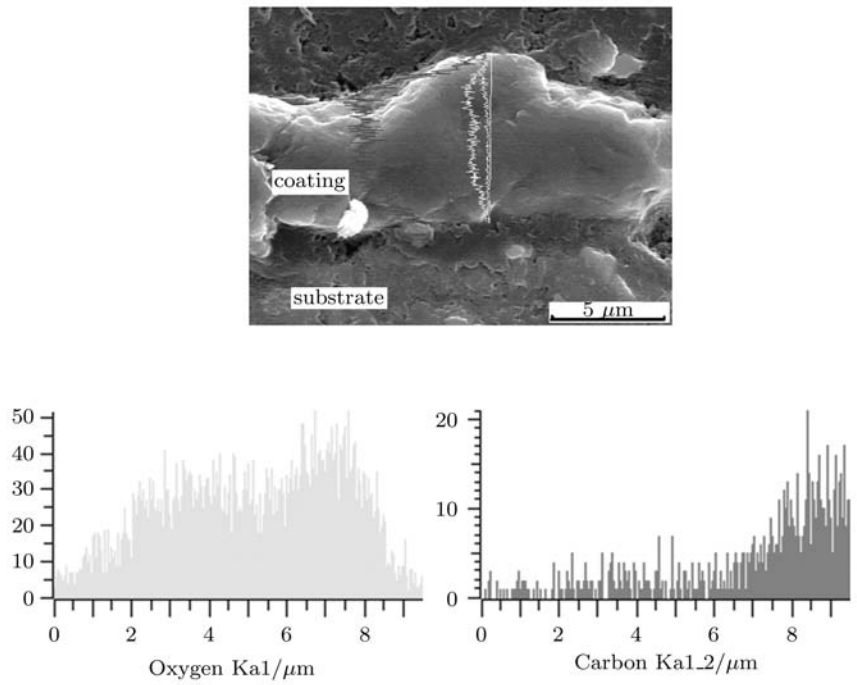



**Fig. 2.** SEM micrographs of (a) graphite powders with average diameter 10 $\mu$m, (b) PEO coating without graphite additives, (c) PEO coating with graphite additives.



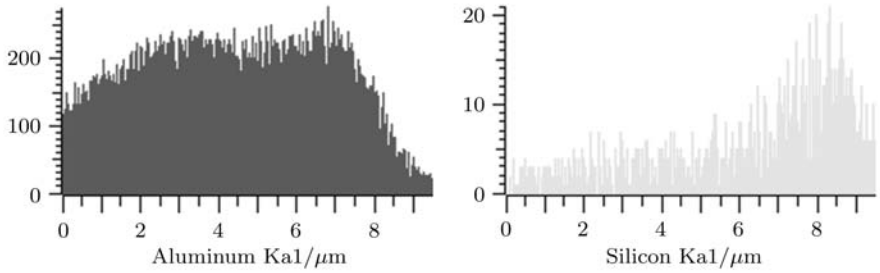



**Fig. 3.** Cross-section morphology and the element distributions across the coating with graphite additives.

### 3.3. EIS characteristics

Experimental impedance spectra collected from Al substrate and the PEO coatings after 10-min immersion in the 3.5-wt% NaCl solution, are presented in the Bode plots in Fig. 4. It can be found that the $|z|$ value of the PEO coating increases greatly compared with that of the metal substrate, which indicates that the corrosion resistance of the substrate is improved by the PEO coatings. Two time constants are shown for the PEO coatings in Fig. 4(b), suggesting the two-layer structure of coatings: the high frequency (HF) range characterizes the properties of the outer layer, while the low frequency (LF) range reveals the properties of the inner layer.[18−20] This is not consistent with the cross-section image of the coating shown above. Since the pores in the coating might be blocked in the polishing process, the results from the EIS spectra are more credible than those obtained from the SEM image.

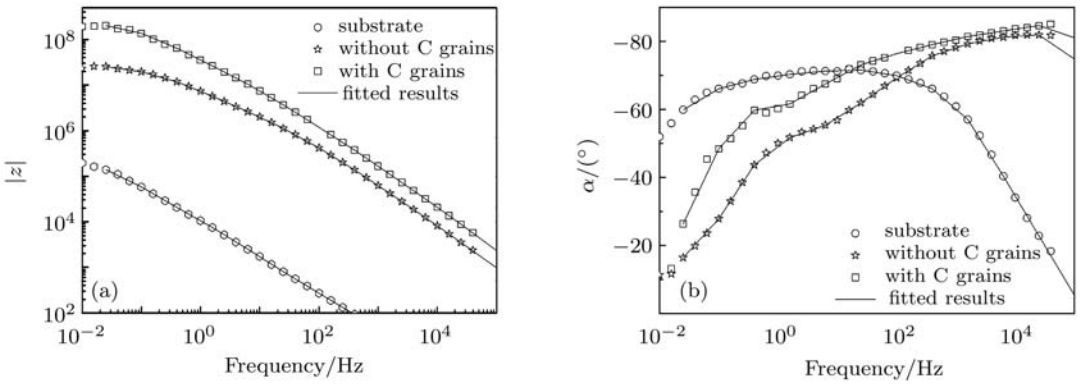



**Fig. 4.** Bode plots of bare aluminum and the PEO coatings.

According to the EIS plots, the typical structure of the PEO coatings[21] and the results given by Liu *et al.*,[22] EIS equivalent circuits of the bare aluminum substrate and the PEO coating are proposed in Figs. 5(a) and 5(b), respectively. For the aluminum substrate, the impedance between reference electrode (SCE) and working electrode is composed of two parts: the impedance of solution and the impedance of bare aluminum, which are characterized by $R_s$ and ($R_a$-$CPE_a$) components, where CPE stands for constant phase element. However, the equivalent circuit for PEO coating consists of three parts: the solution, the outer porous layer and the inner barrier layer. The resistance of the NaCl solution is characterized by $R_s$ which is connected in series with the unit of the composite coating system. The resistance of the outer porous layer is described by the paralleled $R_p$ and the CPE. The magnitude of CPE is $Q_p$, which is composed of two parameters $Q_p - T$ and $Q_p - P$. The inner barrier layer is represented by $R_b$ and $Q_b$ in parallel. According to the equivalent model shown in Fig. 5, the curves in the Bode plots are fitted and the results are presented in Fig. 4 as solid lines passing through the testing data points. The corresponding values of the circuit elements are listed in Table 1.

From Table 1, it can be found that for the PEO coatings with graphite additives, $R_b$ is three orders larger than $R_p$, which further confirms that the coat-

ing is composed of inner barrier and outer porous layers. Compared with the coatings produced in electrolyte without graphite powder additives, the curves (Fig. 4(a)) with graphite additives shift toward the higher frequencies and the phase angles both in the high and low frequencies were larger. Accordingly, both the values of $R_{\rm p}$ and $R_{\rm b}$ are larger than those without graphite additives. These all predict that in the immersion process, for the coating with graphite additives its capacitance is low and resistance is high compared with those for the coating without graphite additives. In addition, this occurs in both the outer porous layer and inner barrier layer. It is well known that because the samples are immersed in the NaCl solution, the solution may infiltrate into the coating. Since the solution has a lower resistance and higher dielectric constant than the air, the penetration leads the capacitance to increase and the resistance to decrease. So it could be inferred that it is more difficult for NaCl solution to infiltrate into the PEO coating with graphite additives. That is to say, the PEO coating becomes denser in both the outer layer and the inner layer. This can be confirmed by the surface morphology (Fig. 2) and element distribution (Fig. 3) of the coating.

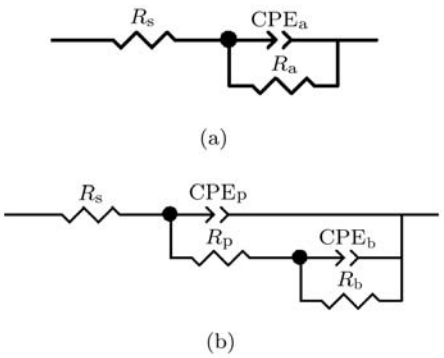



**Fig. 5.** Equivalent circuits for impedance data fitting of (a) Al substrate, (b) PEO coating.

**Table 1.** EIS data simulations for bare aluminium and the PEO coating.

| | $R_{\rm s}/\,\Omega\cdot{\rm cm}^2$ | $Q_{\rm p}-T/10^{-9}$ F·cm$^2$ | $Q_{\rm p}-P$ | $R_{\rm p}/\,\Omega\cdot{\rm cm}^2$ | $Q_{\rm b}-T/10^{-8}$ F·cm$^2$ | $Q_{\rm b}-P$ | $R_{\rm b}/10^7\ \Omega\cdot{\rm cm}^2$ |
|---|---|---|---|---|---|---|---|
| sub | 7.742 | 24062 | 0.77933 | 814000 | — | — | — |
| without C | 99.73 | 5.278 | 0.96003 | 28607 | 6.7913 | 0.54664 | 2.035 |
| with C | 88.54 | 2.437 | 0.960223 | 105160 | 1.3890 | 0.60566 | 18.160 |

## 4. Conclusion

The graphite sealed PEO coatings are studied by SEM and EIS. The results show that in the PEO process, the breakdown voltage is lower when graphite powders are added into the electrolyte. Graphite elements are found to be distributed across the PEO coating and they prefer to be distributed in the surface of the coating. Coating with graphite additives has a two-layer structure, and its inner barrier and outer porous layers are both denser than those of the coating without graphite additives. The result also indicates that EIS is a powerful tool for acquiring the detailed information about the coating structure.

## References


[1] Yerokhin A L, Nie X, Leyland A, Matthews A and Dowey S J 1999 *Surf. Coat. Technol.* **122** 73

[2] Guo H F, An M Z, Xu S and Huo H B 2005 *Thin Solid Films* **485** 53

[3] Gu W C, Lü G H, Chen H, Chen G L, Feng W R, Zhang G L and Yang S Z 2007 *Acta Phys. Sin.* **56** 2337 (in Chinese)

[4] Wang J B, Wu H H, Li Q J, Li Z K, Gu G R, Lü X Y, Zheng W T and Jin Z S 2005 *Chin. Phys.* **14** 2598

[5] Yerokhin A L, Snizhko L O, Gurevina N L, Leyland A, Pilkington A and Matthews A 2003 *J. Phys.* D: *Appl. Phys.* **36** 2110

[6] Wu H H, Wang J B, Long B Y, Long B H, Jin Z S, Wang N D, Yu F R and Bi D M 2005 *Appl. Surf. Sci.* **252** 1545

[7] Jang J, Guo B G, Tian J, Liu H W, Zhou J F and Xu T 2005 *Appl. Surf. Sci.* **252** 345

[8] Xue W B, Wang C, Tian H and Lai Y C 2007 *Surf. Coat. Technol.* **201** 8695

[9] González J A, López V, Bautista A, Otero E and Nóvoa X R 1999 *J. Appl. Electrochem.* **29** 229

[10] Suay J J, Giménez E, Rodríguez T, Habbib K and Saura J J 2003 *Corros. Sci.* **45** 611

[11] Duan H P, Du K Q, Yan C W and Wang F H 2006 *Electrochim. Acta* **51** 2898

[12] Lü G H, Gu W C, Chen H, Feng W R, Khosa M L, Li L, Niu E W, Zhang G L and Yang S Z 2006 *Appl. Surf. Sci.* **253** 2947

[13] Monfort F, Berkani A, Matykina E, Skeldon P, Thompson G E, Habazaki H and Shimizu K 2005 *J. Electrochem. Soc.* **152** C382
[14] Tong H, Jin F and Shen L 2005 *J. Korean Phys. Soc.* **46** S134
[15] Jin F, Chu P K, Tong H H and Zhao J 2006 *Appl. Surf. Sci.* **253** 863
[16] Nie X, Wang L, Konca E and Alpas A T 2004 *Surf. Coat. Technol.* **188–189** 207
[17] Lü G H, Chen H, Gu W C, Feng W R, Li L, Niu E W, Pang H, Zou B and Yang S Z 2009 *Curr. Appl. Phys.* **9** 324
[18] Duan H, Yan C W and Wang F H 2007 *Electrochim. Acta* **52** 3785
[19] Cao C N and Zhang J Q 2002 *An Introduction to Electrochemical Impedance Spectroscopy* (Beijing: Science Press) (in Chinese)
[20] Liu C, Bi Q, Leyland A and Matthews A 2003 *Corros. Sci.* **45** 1257
[21] Xue W B, Wang C, Deng Z W, Chen R Y, Li Y L and Zhang T H 2002 *J. Phys.: Condens. Matter* **14** 10947
[22] Liu J G, Gong G P and Yan C W 2005 *Electrochim. Acta* **50** 3320